An Overview of Synchronization Algorithms for IR-UWB Systems

R. Akbar[1-2] and E. Radoi[1-2]
[1]Université Européenne de Bretagne, France
[2]Université de Brest; CNRS, UMR 3192 Lab-STICC, ISSTB,
6 avenue Victor Le Gorgeu, CS 93837, 29238 Brest cedex 3, France
{Rizwan.Akbar, Emanuel.Radoi} @univ-brest.fr
http://www.lab-sticc.fr

***Abstract*—Ultra wideband (UWB) radio has emerged as an attractive candidate for short-range wireless communications in recent years due to its unique features. However, implementation of UWB radios in order to utilize these features is coupled with some pronounced design challenges. To achieve precise timing synchronization is one of the most crucial task among them and is a key factor to ensure a reliable performance of such systems. In this paper, we present a brief review of IR-UWB synchronization algorithms which are based on either correlation or code matching or energy detection. The performance is then analyzed under realistic propagation environment that takes into account the severe multipath, inter-frame interference (IFI) & inter-symbol interference (ISI) and multi-user interference (MUI).**

***Index Terms*—Impulse radio ultra wideband (IR-UWB), time hopping (TH), synchronization, dirty template, asymmetric modulation, orthogonal code.**

I. Introduction

Ultra wideband (UWB) radio has been drawing plentiful attention among researchers since February 2002 when Federal Communication Commission (FCC) allocated a large swathe of 7.5GHz spectrum in 3.1-10.6 GHz range with extremely low power spectral density of -41.25 dBm/MHz for UWB communications. Impulse radio UWB (IR-UWB) is one possible solution to implement UWB systems, characterized by data transmission using trains of nanoseconds level pulses. The interest in IR-UWB is attributed to many unique features such as its ability to coexist with existing narrowband systems in underlay mode, simple baseband transceiver, low probability of interception and detection, high ranging resolution and ability to exploit rich multipath diversity [1].

The aforementioned attractive features, however, come at a cost of equally demanding design challenges and precise synchronization is one of them. The stringent timing requirements pose a major challenge to the deployment of IR-UWB and timing accuracy is fundamental to ensure a satisfactory performance of such systems. Even a slight misalignment at the order of nanoseconds can severely degrade the system performance [2], [3], especially if correlation based coherent receiver is opted. Although synchronization is a tough task to accomplish in any communication system, it becomes much more challenging in UWB due to the need of very high accuracy and that too using low-power impulsive UWB pulses. The unknown frequency selective channels induce inter-symbol interference (ISI) which further intricate the task [4].

Due to these reasons, several timing algorithms have been proposed in past. A number of algorithms treat timing as a part of channel estimation and aim at joint estimation of timing and channel taps [5]–[7]. In [5], this is done using maximum-likelihood (ML) criterion . A formidably high sampling rate upto several GHz along with suboptimal estimation in closely spaced multipaths raise concerns over its implementation. A least squared (LS) based method is presented in [6] which looks for the minimum of Euclidean distance between received signal samples and a local replica of their noiseless components. However, it involves two dimensional searching along with very high sampling rate. Besides, it may require very fast analog-to-digital converters (ADC) as it is a fully digital approach. Another joint channel estimation and synchronization scheme developed in [7] employs subspace method. The timing estimation is converted to a harmonic retrieval problem and is solved using subspace analysis. The implementation complexity involved in subspace analysis along with possible ill-conditioned Vandermonde systems in closely spaced multipaths limits its application to realistic UWB scenarios. Several other algorithms based on low complexity ML [8], cyclostationarity [9] and first-order statistics [10] have also been studied, however most of them require certain assumptions such as absence of time-hopping (TH) codes, absence or known multipath, no inter-frame/inter-symbol interference (IFI/ISI) etc, thus impractical in real UWB settings.

In this paper, we will focus on three methods, flexible enough to be implemented digitally or in analog form, thus appeasing the implementation complexity due to high sampling rate. They are correlation based timing acquisition proposed in [11], orthogonal code matching based method in [12] and energy detection based method presented in [4]. These methods not only relieve the sampling rate requirements but are also functional in most of the practical UWB environments. Section II describes signal format and preliminaries. In section III, overview of synchronization algorithms is given. Sections IV provides comparative analysis about implementation constraints of studied algorithms. Finally, simulation results are provided in section V to corroborate the discussion while conclusions are summarized in section VI.

II. System Model and preliminaries

The transmitted signal in IR-UWB radio for point-to-point link equipped with symbol periodic time-hopping (TH) codes can be expressed as

$$s(t) = \sum_n a(n) p_T(t - nT_s) \tag{1}$$

where $p_T(t) = \sum_{j=0}^{N_f-1} p(t - jT_f - c_jT_c)$ is symbol-long waveform of duration $T_s = N_fT_f$ consisting of N_f frames each of duration T_f and $\{a(n)\}$'s are information-bearing symbols taking values ± 1 with equal probability. An ultra-short UWB waveform $p(t)$ of duration $T_p \ll T_f$ is transmitted one per frame which means that N_f waveforms are used to represent one data symbol. These UWB pulses are time shifted by integer multiples of chip duration $T_c = \lfloor T_f/N_c \rfloor$ in each frame by user-specific pseudo-random TH code $\{c_j\}_{j=0}^{N_f-1} \in [0, N_h - 1]$ with $N_h \leq N_c$, where N_c is the number of chips per frame satisfying $T_f = N_cT_c$. These TH codes serve dual purpose of spectral smoothing along with enabling multiple access.

The impulse response of L-tap multipath UWB channel can be denoted as $h(t) = \sum_{l=0}^{L-1} \lambda_l \delta(t - \tau_l)$, where $\{\lambda_l, \tau_l\}_{l=0}^{L-1}$ are channel path gains and delays respectively, satisfying $\tau_l < \tau_{l+1}$, $\forall\, l$. These channel coefficients are assumed invariant over one transmission burst due to quasi-static nature of UWB channel, but are allowed to vary across bursts. Typically, UWB channel's rms delay spread (τ_{rms}) satisfies: $\tau_{rms} \gg T_p$, thus inducing ISI, and channel's coherence time (T_{coh}) satisfies: $T_{coh} \gg T_p$, resulting in slow fading. Letting the relative path delay as $\tau_{l,0} := \tau_l - \tau_0$, the signal at the receiving end is the convolution $s(t) \star h(t - \tau_0)$ in the presence of AWGN noise $w(t)$ with double-sided power spectral density $N_0/2$, given by

$$r(t) = \sum_n a(n) p_R(t - nT_s - \tau_0) + w(t) \tag{2}$$

where $p_R(t) = \sum_{j=0}^{N_f-1} g(t - jT_f - c_jT_c)$ is the aggregate received symbol waveform of duration T_R, with $g(t) = \sum_{l=0}^{L-1} \lambda_l p(t - \tau_{l,0})$ representing single UWB dispersed pulse of duration T_g. Evidently, by selecting $(N_h - 1)T_c + T_p + \tau_{L,0} \leq T_f$, we can avoid both IFI and ISI, while choosing $T_p + \tau_{L,0} \leq T_f$ and $c_{N_f-1} = 0$ will ensure again no ISI but will allow IFI. Our objective is to estimate the timing offset τ_0 in the absence of any knowledge about transmitted sequence and multipath channel.

III. Synchronization Algorithms

In this section, we outline the basic working principle of three IR-UWB synchronization schemes and their complexity and limitations will be discussed in next section.

A. Timing with Dirty Template (TDT)

One simplest approach for synchronization in impulse radio is based on match-filtering the received signal with a locally generated "clean template" and peak-picking the correlation samples. Evidently, the reference template must encompass multipath channel effect which is unknown at synchronization stage, thus needing a cumbersome task of channel estimation. A scheme, known as timing with dirty templates (TDT), was proposed in [11] to tackle this issue by utilizing pair of successive symbol long segments of $r(t)$, where one segment serves as template for the other. These segments are termed as "dirty templates" because they are i) noisy, ii) distorted by unknown channel and iii) subject to unknown timing offset τ_0. Knowledge about multipath channel and TH codes becomes unnecessary as this information is already embedded in dirty templates and thus improves energy capture.

The basic idea behind TDT hinges upon finding the maximum of square of symbol-rate samples, obtained by simple integrate-and-dump operation performed on the products of dirty templates. Both NDA and DA variants of TDT are proposed in [11] where the former are bandwidth efficient while the latter enjoy fast synchronization. In the absence of MUI and ISI, the timing offset τ_0 can be estimated in NDA-TDT as

$$\begin{aligned} \hat{\tau}_0 &= \arg \max_{\tau \in [0, T_s)} J_{nda}(\tau) \\ J_{nda}(\tau) &= \frac{1}{K} \sum_{k=1}^{K} \left(\int_{2kT_s}^{(2k+1)T_s} r(t+\tau) r(t+\tau-T_s) dt \right)^2 \end{aligned} \tag{3}$$

where K is the number of symbol-long pairs. To grasp the gist of TDT, first the symbol-rate samples are obtained by integrate-and-dump operation as

$$x_k(\tau) = \int_0^{T_s} r(t + 2kT_s + \tau) r(t + (2k-1)T_s + \tau) dt \tag{4}$$

$\forall k \in [1, +\infty)$, $\tau \in [0, T_s)$. Ignoring the noise brevity, the received waveform can be represented using (2) as

$$r(t + kT_s + \tau) = \sum_n a(n) p_R(t - T_s + \tau_0 + kT_s + \tau) \tag{5}$$

Assuming that the non-finite support T_R of $p_R(t)$ is upper bounded by symbol duration T_s to avoid ISI, it is obvious that only two adjacent values of n will contribute nonzero summands in (5). Thus (5) is simplified as

$$r(t + kT_s + \tau) = a(k-1) p_R(t + T_s - \tilde{\tau}_0) + a(k) p_R(t - \tilde{\tau}_0) \tag{6}$$

$\forall t$, $\tau \in [0, T_s)$, where $\tilde{\tau}_0 := [\tau_0 - \tau]_{\bmod T_s}$. Substituting (6) in (4), we get $x_k(\tau) = a(2k-1)[a(2k-2)\varepsilon_A(\tilde{\tau}_0) + a(2k)\varepsilon_B(\tilde{\tau}_0)$ where $\varepsilon_A(\tilde{\tau}_0) = \int_{T_s - \tilde{\tau}_0}^{T_s} p_R^2(t) dt$ and $\varepsilon_B(\tilde{\tau}_0) = \int_0^{T_s - \tilde{\tau}_0} p_R^2(t) dt$. The mean square of $x_k(\tau)$ can be written as

$$\begin{aligned} \mathrm{E}\{x_k^2(\tau)\} &= \varepsilon_A^2(\tilde{\tau}_0) + \varepsilon_B^2(\tilde{\tau}_0) \\ &= \frac{1}{2} \left[\{\varepsilon_A(\tilde{\tau}_0) + \varepsilon_B(\tilde{\tau}_0)\}^2 + \{\varepsilon_A(\tilde{\tau}_0) - \varepsilon_B(\tilde{\tau}_0)\}^2 \right] \end{aligned} \tag{7}$$

Now observe that $\varepsilon_A(\tilde{\tau}_0) + \varepsilon_B(\tilde{\tau}_0) = \int_0^{T_s} p_R^2(t) dt = \varepsilon_R$ is the constant energy of the aggregate template and does not contain any information. However, the energy difference $\varepsilon_B(\tilde{\tau}_0) - \varepsilon_A(\tilde{\tau}_0)$ is uniquely maximized at $\tilde{\tau}_0 = 0$ or equivalently $\tau = \tau_0$, since $\varepsilon_A(\tilde{\tau}_0)$ is minimized at $\tilde{\tau}_0 = 0$ and $\varepsilon_B(\tilde{\tau}_0)$

is maximized at $\tilde{\tau}_0 = 0$, by definition. Thus, $\mathrm{E}\{x_k^2(\tau)\}$ can be considered as a sufficient criterion for estimating τ_0. Replacing ensemble mean with its sample mean estimator using K pairs of symbol long received segments will eventually return the objective function $J_{nda}(\tau)$ of (3).

To speed up acquisition, a data-aided (DA) variant of NDA-TDT is possible using training sequence of $a(n) = (-1)^{\lfloor \frac{n}{2} \rfloor}$. This training pattern will reduce ensemble mean in (7) to $\mathrm{E}\{x_k^2(\tau)\} = [\varepsilon_A(\tilde{\tau}_0) - \varepsilon_B(\tilde{\tau}_0)]^2$ in noiseless case. Thus, in principle, as few as four symbols are sufficient for reliable estimation at high SNR. The performance in DA-TDT can be further improved by swapping the order of correlation and averaging in (3), thus developing the following criterion

$$\hat{\tau}_0 = \arg \max_{\tau \in [0, T_s)} J_{da}(\tau)$$
$$J_{da}(\tau) = \left(\int_0^{T_s} \tilde{r}(t+\tau)\tilde{r}(t+\tau-T_s)dt \right)^2 \quad (8)$$

where

$$\tilde{r}(t) = (-1)^{\lfloor t/2T_s \rfloor} \bar{r}(t)_{\bmod 2T_s}$$

with $\bar{r}(t) = (1/K)\sum_{k=1}^{k}(-1)^k r(t+2kT_s)$, $t \in [0, 2T_s]$. This criterion provides best performance because using $\tilde{r}(t)$ in cost function $J_{da}(\tau)$ will reduce power spectral density of AWGN term to $N_0/2K$, thanks to averaging.

B. Timing with Code Matching (TCM)

The methods in this class are based on exploiting the discriminative nature of well-designed polarity codes. The proposal in [12] relies on code matching and signal aggregation of one frame-long segments followed by energy detection. The transmitted symbol is multiplied with a polarity code $\{d_j\}_{j=0}^{N_f-1}$, resulting in $p_T(t) = \sum_{j=0}^{N_f-1} d_j p(t - jT_f - c_jT_c)$ and consequently $p_R(t) = \sum_{j=0}^{N_f-1} d_j g(t - jT_f - c_jT_c)$. The estimate of τ_0 is obtained by the optimization given as

$$\hat{\tau}_0 = \arg \max_{\tau \in [0, T_s)} J_{tcm}(\tau)$$
$$J_{tcm}(\tau) = \sum_{k=1}^{K} \int_0^{T_I} \left| \sum_{j=0}^{N_f-1} d_j g_r(t) r(t + t_{k,j} + \tau) \right|^2 dt \quad (9)$$

where $t_{k,j} = kT_s + jT_f + c_jT_c$, $d_j g_r(t)$ is the correlation template for j^{th} frame and T_I is the integration interval. In words, the idea is simply to take frame long segments of same symbol, time shift them using TH codes and bi-polarize them by d_j at transmitter. At receiver, the synchronizer compensates for TH codes using *a-priori* knowledge and polarity change due to d_j followed by superimposition. Due to judiciously designed polarity code, this superimposition will result in constructive sum only if $\tau = \tau_0$ and consequently $J_{tcm}(\tau)$ will capture maximum energy given by $J_{tcm}(\tau_0) = KN_f^2 \int_0^{T_g} g^2(t)dt$. Otherwise, if $\tau = \tau_0$, this superimposition will result in destructive addition, thus capturing much smaller energy.

It is clear from (9) that the accuracy of estimation depends on both $d_j g_r(t)$ and value of T_I, which determine the amount of energy captured in each integration. Although maximum SNR is achieved at receiver by setting $g_r(t) = g(t)$, selecting $g_r(t) = 1$ can also ensure a reliable estimation while simplifying the implementation at the same time. This effectively reduces correlation template $d_j g_r(t)$ to d_j, thus the suitable design of polarity codes is non-trivial for the algorithm to perform well. These codes must satisfy the periodic autocorrelation functions (ACF) defined as

$$R_d^+[n] = \frac{1}{N_f} \sum_{j=0}^{N_f-1} d_j d_{(j+n)_{\bmod N_f}}$$
$$R_d^-[n] = \frac{1}{N_f} \left(\sum_{j=0}^{N_f-n-1} d_j d_{j+n} - \sum_{j=N_f-n}^{N_f-1} d_j d_{(j+n)_{\bmod N_f}} \right) \quad (10)$$

There are many codes available which satisfy the positive periodic ACF $R_d^+[n]$ such as Barker codes, M-sequences etc. However, due to blind synchronization, the two consecutive BPSK symbols may be different, thus the code design must also take into account the negative periodic ACF $R_d^-[n]$. A minimax criterion to design these codes along with some optimal codes for certain values of N_f are listed in [12].

The other important parameter in (9) is the value of T_I that can be set as T_g ideally, if information about maximum channel delay spread is known to receiver. Otherwise, T_I can be replaced by an upper bound on maximum dispersion or even by $T_f - N_h T_c$.

C. Timing with Energy Detection (TED)

Low-complexity synchronization is possible via energy detection based methods which rely on exploiting the portion of received signal with significant energy, introduced specifically to enable synchronization. An interesting ISI and multi-user interference (MUI) resilient method was proposed in [4], which relies on intermittent transmission of nonzero mean symbols deliberately introduced by changing the modulation constellation at transmitter. During synchronization phase, one asymmetric BPSK symbol taking values $(\theta, -1)$ equiprobably with nonzero mean: $\mu = 0.5\theta + 0.5(-1)$, with $\theta > 1$, is transmitted for every $(M-1)$ zero mean symbols where $M = \lceil T_R/T_s \rceil + 1$ is channel delay spread dependent integer. Under the condition that AWGN and MUI are zero mean, the timing offset τ_0 can be estimated by

$$\hat{\tau}_0 = \arg \max_{\tau \in [0, MT_s)} J_{ted}(\tau)$$
$$J_{ted}(\tau) = \int_0^{T_R} \left| \bar{r}((t+\tau)_{\bmod MT_s}) \right|^2 dt \quad (11)$$

where $\bar{r}(t) = \frac{1}{K}\sum_{k=0}^{K-1} r(t + kMT_s)$, $t \in [0, MT_s]$ is the sample mean estimator of $r(t)$ across K segments each of size MT_s. This mean of $r(t)$ will comprise of zero guards of size $MT_s - T_R \geq T_s$, which will be exploited by energy detector to estimate τ_0. This in-turn implies another condition for the algorithm to function properly which is that there should be no interval larger than T_s where $p_R(t) = 0$ over its support $[0, T_R]$. This can be met by choosing symbol

period $T_s \geq \Delta\tau_{\max} - \left[(N_f-1)T_f + c_{N_f-1}T_c + T_g\right]$, where $\Delta\tau_{\max} \geq \max_{l\in[1,L)}(\tau_l - \tau_{l-1})$ is the maximum successive channel delay difference. If this condition is not respected, then there will be multiple zero guards in $\bar{r}(t)$ rendering the algorithm non-functional. The condition of zero mean MUI is satisfied if only one user takes the responsibility of synchronization while others are transmitting zero mean interfering symbols, which is usually the case in ad-hoc networks.

IV. Implementation Constraints Analysis

Regarding implementation complexity, the methods described in previous section are particularly interesting as they can be computed either digitally or in analog form. All of these methods needs symbol-rate sampling, thus relaxing the subpulse rate sampling needed in [5], [6]. Analog delays to shift received signal segments by $2T_s$ or $t_{k,j}$ or MT_s are required in analog approaches which can be challenging. On the other hand digital domain implementation needs very high sampling rate in UWB regime. Nevertheless, one can adopt according to available resources, thus providing flexibility. As far maximization algorithms itself, each objective function needs a serial search which is not efficient and result in increased mean synchronization time. There are other search strategies possible, however their reduced mean synchronization time comes at a cost of lesser performance and rather strict conditions. Due to prohibitive complexity involved in linear search, usually the objective function is evaluated over a grid of equispaced $N_\delta = \lfloor T_s/T_\delta \rfloor$ discrete bins each of duration T_δ to estimate $\hat{\tau}_0 = \hat{n}T_\delta$. It is worth mentioning that these algorithms can synchronize at any desired resolution and search is only constrained by the affordable complexity.

As for the assumptions or *a-priori* knowledge are concerned, NDA-TDT is ideal as it needs no information whatsoever about transmitted signal. But its operation is quite limited and not applicable in ISI and MUI scenarios. DA-TDT shows resilience to MUI but not to ISI. *A-priori* information about user's TH codes and also about τ_{max} are needed to select optimal value of T_I in TCM. It has been seen by simulations that when $T_I > T_g$, there is a plateau corresponding to same maximum in cost function $J_{tcm}(\tau)$, thus introducing ambiguity, while when $T_I < T_g$ the maximum may drift from original τ_0. So value of T_I has a considerable impact on synchronization accuracy in TCM. Same is true for TED which also needs information about τ_{max} and at least about c_{N_f-1} to select T_R. It is worth stressing here that T_R is not only needed by synchronizer to select integration region but is also required by transmitter to select integer M which is used to decide about symmetric and asymmetric modulated symbols. Another disadvantage of TED is the aggravate SNR at receiver due to asymmetric modulation, which will deteriorate BER performance significantly during synchronization phase.

V. Simulations and Comparisons

In this section, we will provide some preliminary simulation results to validate our discussion and will analyze how these methods behave in different operating conditions. A UWB pulse generated using B-spline based approach [13] is employed in simulations, which utilizes FCC mask efficiently. The channel model used is indoor multipath channel proposed by IEEE 802.15.3a working group [14]. Timing offset τ_0 is randomly generated from a uniform distribution over $[0, T_s)$ at each Monte Carlo trial. We have focused only on frame-level coarse synchronization to keep the simulation time within acceptable limit i.e. we set $T_\delta = T_f$. Each symbol consists of $N_f = 13$ frames. The remaining parameters are selected according to different operating conditions which are explained as follows :

Test A. IFI/ISI Free: To avoid any interfernce among frames and symbols, we select $T_c = T_p = 1.28$ns, $N_c = 20$ resulting in frame duration $T_f = 25.60$ns and $N_h = 5$. The channel used is the indoor CM1, having rms delay spread $\tau_{rms} = 5$ns and truncated beyond $T_f - N_h T_c$ to avoid IFI/ISI.

Test B. IFI Present: Next we consider the case which includes IFI but no ISI. This is achieved in simulations by selecting $N_h = 10$ and $c_{N_f-1} = 0$. The channel in this case is truncated beyond $T_f - T_c$.

Test C. ISI Present: To allow ISI, we consider a much severe case by selecting CM4 channel of IEEE 802.15.3a standard, which has $\tau_{rms} = 25$ns. The channel is truncated beyond 50ns and energy normalized, T_f is reduced to 10ns and we avoid TH codes to observe the impact of ISI only.

Test D. MUI Present: We return to the original setting of Test A, but this time we assume that there are two interfering users also present in the system. The interfering users transmit at same power as desired user and employ different polarity and TH codes.

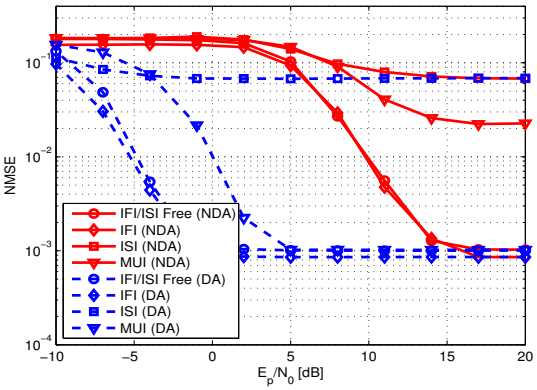

Figure 1. Performance of TDT synchronizer in both NDA and DA mode with $K = 64$ pairs of dirty tempaltes.

The normalized MSE (w.r.t T_s^2) performance of three methods under these scenarios is plotted as a function of E_p/N_0 (where E_p is the energy of basic UWB pulse) in Figs. 1, 2 and 3. The floor in each figure is due to coarse synchronization employed and will alleviate with increased resolution. One can observe the significant improvement in performance using DA version of TDT in Fig. 1. The performance under Test A. and B. is quite similar. This is due to fact that due to smaller

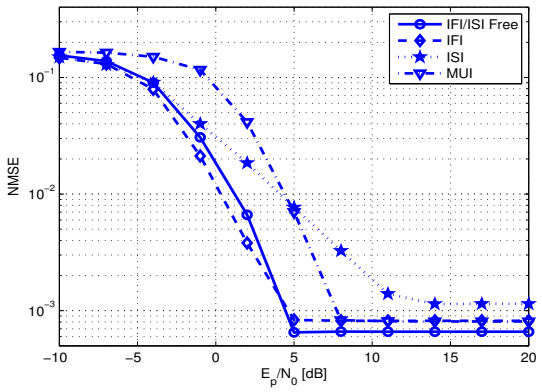

Figure 2. Performance of TCM synchronizer with $K = 64$ symbols.

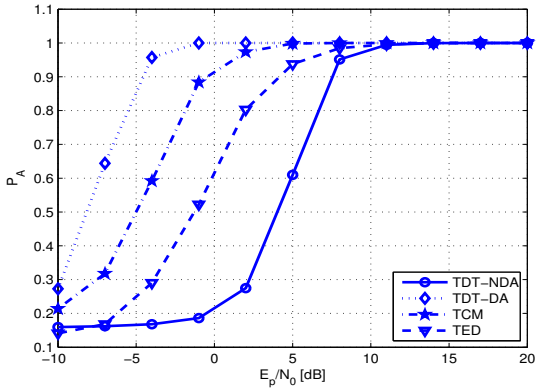

Figure 4. Comparison of TDT, TCM & TED in terms of Probability of Acquisition in IFI/ISI Free scenario.

delay spread of CM1, most of channel energy resides in the same frame and out-of-frame energy affecting the next frame is not significant one. As discussed, NDA can not estimate timing offset in ISI and MUI scenarios whereas DA does estimate under MUI but with reduced performance. However, even DA version can not estimate in the presence of ISI. We

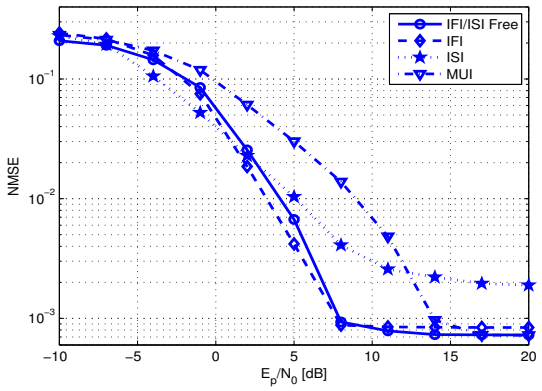

Figure 3. Performance of TED synchronizer with $K = 64$ symbols of size MT_s.

have assumed that information about channel delay spread was available, so both T_I and T_R are set to their optimal values in TCM and TED respectively. The curves in Figs. 2 and 3 show that both algorithms are functional in all cases, however peformance is reduced significantly in ISI for both algorithms. Fig. 4 provides a relative comparison of three techniques under simplest case of no IFI/ISI in terms of probability of acquisition, defined as the probability that $|\hat{\tau}_0 - \tau_0| \leq T_f$. DA-TDT performs best among all, however it will incur rate loss due to training sequence. Among blind methods, code matching certainly outperforms the rest.

VI. Conclusions

In this paper, we have presented an overview of few synchronization algorithms employed in IR-UWB. These methods have formed the basis of many new schemes proposed recently for acquisition, thus understanding them will help to further dwell into the rather challenging task of synchronization. The working principle along with their limitations are presented and simulation results are provided to validate the discussion.

References

[1] L. Yang and G. B. Giannakis, "Ultra-wideband communications: An idea whose time has come," *IEEE Sig. Process. Mag.*, vol. 21, no. 6, pp. 26–54, Nov. 2004.

[2] Z. Tian and G. B. Giannakis, "BER sensitivity to mistiming in ultra-wideband impulse radios- part I: Nonrandom channels," *IEEE Trans. on Sig. Process.*, vol. 53, no. 4, pp. 1550–1560, April 2005.

[3] N. He and C. Tepedelenlioglu, "Performance analysis of non-coherent UWB receivers at different synchronization levels," *IEEE Trans. on Wireless Commun.*, vol. 5, no. 6, pp. 1266–1273, June 2006.

[4] X. Luo and G. B. Giannakis, "Low-complexity blind synchronization and demodulation for (ultra-)wideband multi-user ad hoc access," *IEEE Trans. on Wireless Commun.*, vol. 5, no. 7, pp. 1930–1941, July 2006.

[5] V. Lottici, A. D'Andrea, and U. Mengali, "Channel estimation for ultra-wideband communications," *IEEE Journal on Sel. Areas in Commun.*, vol. 20, no. 9, pp. 1638–1645, 2002.

[6] C. Carbonelli and U. Mengali, "Synchronization algorithms for UWB signals," *IEEE Trans. on Commun.*, vol. 54, no. 2, pp. 329–338, 2006.

[7] I. Maravic and M. Vetterli, "Low-complexity subspace methods for channel estimation and synchronization in ultra-wideband systems," in *Proc. of Intl. Workshop on Ultra-Wideband (IWUWB)*, Oulu, Finland, 2003.

[8] Z. Tian and V. Lottici, "Low-complexity ML timing acquisition for UWB communications in dense multipath channels," *IEEE Trans. on Wireless Commun.*, vol. 4, no. 6, pp. 3031–3038, 2005.

[9] L. Yang, Z. Tian, and G. B. Giannakis, "Non-data aided timing acquisition of ultra-wideband transmissions using cyclostationarity," in *Proc. of IEEE Intl. Conf. on Acoustic, Speech and Signal Process. (ICASSP)*, Hong Kong, China, Apr. 2003, pp. 121–124.

[10] Z. Wang and X. Yang, "Ultra wide-band communications with blind channel estimation based on first-order statistics," in *Proc. of IEEE Intl. Conf. on Acoustic, Speech and Signal Process. (ICASSP)*, Montreal, Canada, May 2004, pp. 529 – 532.

[11] L. Yang and G. B. Giannakis, "Timing ultra-wideband signals with dirty templates," *IEEE Trans. on Commun.*, vol. 53, no. 11, pp. 1952–1963, Nov. 2005.

[12] Y. Ying, M. Ghogho, and A. Swami, "Code-assisted synchronization for UWB-IR systems: Algorithms and analysis," *IEEE Trans. on Sig. Process.*, vol. 56, no. 10, pp. 5169–5180, Oct. 2008.

[13] M. Matsuo, M. Kamada, and H. Habuchi, "Design of UWB pulses based on B-splines," in *proc. IEEE Intl. Symp. on Circuits and Systems*, Japan, May 2005, pp. vol. 6, pp. 5425–5428.

[14] J. R. Foerster, M. Pendergrass, and A. F. Molisch, "A channel model for ultrawideband indoor communication," *MERL (Mitsubishi Electric Research Laboratory) Report TR-2003*, vol. 73, 2003.